Acceleration in European Mean Sea Level? A New Insight Using Improved Tools

Author: Watson, Phil J.

Source: Journal of Coastal Research, 33(1) : 23-38

Published By: Coastal Education and Research Foundation

URL: https://doi.org/10.2112/JCOASTRES-D-16-00134.1

Journal of Coastal Research	33	1	23–38	Coconut Creek, Florida	January 2017

Acceleration in European Mean Sea Level? A New Insight Using Improved Tools

Phil J. Watson

School of Civil and Environmental Engineering
University of New South Wales
Sydney, NSW 2052, Australia
philwatson.slr@gmail.com

ABSTRACT

Watson, P.J., 2017. Acceleration in European mean sea-level? A new insight using improved tools. *Journal of Coastal Research,* 33(1), 23–38. Coconut Creek (Florida), ISSN 0749-0208.

Research into sea-level rise has taken on particular prominence in more recent times owing to the global threat posed by climate change and the fact that mean sea level and temperature remain the key proxies by which we can measure changes to the climate system. Under various climate change scenarios, it has been estimated that the threat posed by the effects of sea-level rise might lead to annual damage costs across Europe on the order of €25 billion by the 2080s. European mean sea-level records are among the best time series data available globally by which to detect the presence of necessary accelerations forecast by physics-based projection models to elevate current rates of global sea-level rise ($\approx$3 mm/y) to anywhere in the vicinity of 10–20 mm/y by 2100. The analysis in this paper is based on a recently developed analytical package titled "msltrend," specifically designed to enhance estimates of trend, real-time velocity, and acceleration in the relative mean sea-level signal derived from long annual average ocean water level time series. Key findings are that at the 95% confidence level, no consistent or compelling evidence (yet) exists that recent rates of rise are higher or abnormal in the context of the historical records available across Europe, nor is there any evidence that geocentric rates of rise are above the global average. It is likely a further 20 years of data will distinguish whether recent increases are evidence of the onset of climate change–induced acceleration.

ADDITIONAL INDEX WORDS: *Climate change, velocity, improved measuring approaches*.

INTRODUCTION

Climate change presents formidable social, environmental, and economic challenges for a growing global population. In particular, the threat posed by a projected rise in mean sea level will be profound (McGranahan, Balk, and Anderson, 2007; Nicholls and Cazenave, 2010) unless extensive adaptation responses are successfully implemented. The development and utilisation of coastal zones has greatly increased during the recent decades, and coasts are undergoing tremendous socioeconomic and environmental changes, a trend that is expected to continue into the future (Neumann *et al.,* 2015). Global analysis suggests that coastal population growth and urbanisation rates are outstripping the demographic development of the hinterland, driven by rapid economic growth and coastward migration (McGranahan, Balk, and Anderson, 2007; Neumann *et al*., 2015; Smith, 2011).

Based on population assessments in 2000, it was estimated that the global population living within the low elevation coastal zone (LECZ, <10 m above mean sea level) was on the order of 625 million, of which 50 million were estimated to reside in Europe (Neumann *et al.,* 2015).

The ClimateCost Project undertaken for the European Union (Watkiss, 2011) provides a sobering economic appraisal of the threat from sea-level rise and the costs and benefits of adaptation over the course of the 21st century. For example, it is estimated that under a medium to high greenhouse gas emission scenario (A1B; Meehl *et al.,* 2007), flooding along with other effects of sea-level rise (*e.g.,* shoreline recession) will lead to annual damage costs across Europe of up to €11 billion for the 2050s, rising to €25 billion by the 2080s (Brown *et al.,* 2011). Flooding more generally will of course be substantially exacerbated by forecast sea-level rise into the future, foreboding an increasingly ominous threat from natural disasters (Watson, 2016c).

Improved understanding of how and when climate change effects will occur and evolve over time will be critical to developing robust strategies to adapt and minimise risks (Watson, 2016a). The prominence of the climate change issue has placed more emphasis on examination of the extensive global repository of relative mean sea-level records (Holgate *et al.,* 2012), which, along with temperature and carbon dioxide, remain the key proxy data sets used to monitor and quantify changes in the global climate system (Watson, 2016c). In particular, there has recently been renewed, energetic scientific discussion in the literature over the prospect of a measurable acceleration in ocean water level records, a feature central to physics-based projection models that are built upon the current knowledge of climate science (IPCC, 2013).

Some 28 of the 30 longest records in the Permanent Service for Mean Sea Level (PSMSL) global data holdings are European, extending as far back as 1807 (Brest, France). Such records provide the world's best time series data with which to examine how kinematic properties of the trend might be changing over time. This paper supplements the detailed analysis of the long U.S. records (Watson, 2016c) using the

DOI: 10.2112/JCOASTRES-D-16-00134.1 received 31 July 2016; accepted in revision 9 August 2016; corrected proofs received 25 September 2016; published pre-print online 21 October 2016.

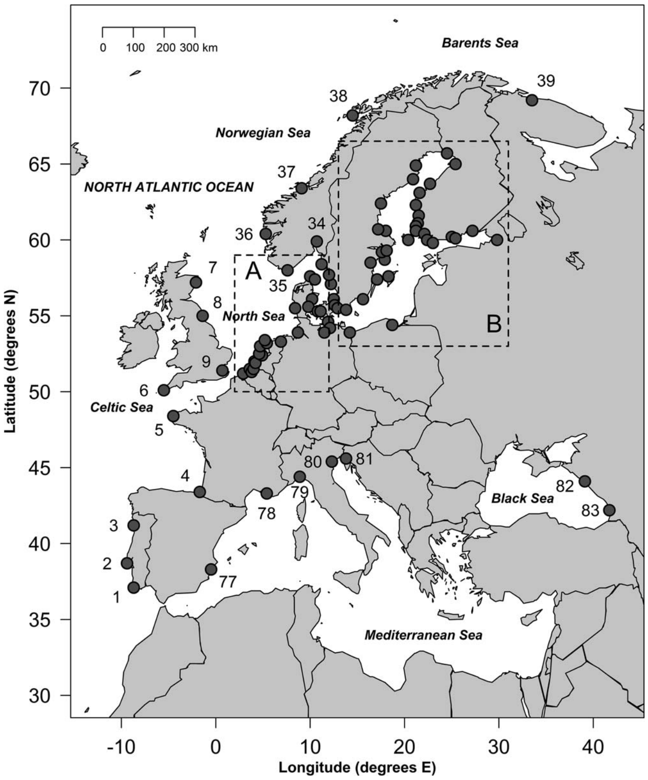

Figure 1. Location of tide gauge records analysed for this study. Each record is denoted by a "Station ID" with further details provided in Table 1. Refer to Figures 2 and 3 for insets A and B, respectively.

same analytical framework and methodology, but applied to the extensive network of European tide gauge records.

Specifically, the paper provides an updated appraisal of acceleration in mean sea-level records around Europe through use of a recently developed analytical package titled "msltrend" (msltrend, 2016) within the R Project for Statistical Computing (R Development Core Team, 2015). The msltrend package has been specifically designed to enhance substantially estimates of trend, real-time velocity, and acceleration in relative mean sea level derived from contemporary ocean water level data sets based on unprecedented time series research, development, and analysis (see "Background" in Watson, 2016c).

The outputs of this research tool provide a more consistent, transparent appraisal of acceleration in mean sea-level records around Europe; overcoming many of the evident shortcomings from the wide body of scientific literature on this topic, which are discussed in detail in Watson (2016c).

Physical Setting

Whilst the extensive quantum of good-quality European relative mean sea-level time series data sets are invaluable for sea-level research, one must also have an understanding of the complex geophysical (and other) factors embedded within the data. The study area (Figure 1) encompasses coastlines on major waterbodies as follows.

North Atlantic Ocean

Between the Strait of Gibraltar, Spain, along the open coast to Murmansk Oblast in the Barents Sea, this area includes the adjacent waterbodies of the Gulf of Cadiz, Bay of Biscay, English Channel, Celtic Sea, Irish Sea, North Sea, Kattegat, and Norwegian Sea.

Mediterranean Sea

This semienclosed waterbody of approximately 2.5 million km^2 is connected to the Atlantic Ocean via the Strait of Gibraltar, which narrows to a mere 13 km. Owing to this constriction, the tides are low compared with that of the Atlantic (Pugh, 1996). The Mediterranean Sea is divided into two large basins separated by the Sicilian Channel and the Messina Strait, with both basins extending to depths of >4 km in places (Arabelos *et al.,* 2011). The Mediterranean is connected to the Black Sea via the Strait of Bosporus and artificially to the Red Sea via the Suez Canal. Some of Europe's largest rivers drain directly or indirectly into the Mediterranean, including the Po (Italy), Ebro (Spain), and Rhône (France), as well as the African Nile (Egypt).

Black Sea

The world's largest inland sea covers an area of 436,000 km^2 exchanging water with the Mediterranean Sea via the Bosporus and Dardanelles straits (Avsar *et al.,* 2016) and the Sea of Azov through the Kerch Strait (Stanev, 2005). At any given time, the level of the Black Sea is principally governed by complex interrelationships between the local water budget (precipitation *vs*. evaporation), eustatic sea-level variations and water exchange through the straits, and continental discharges onto the northern coast via the Danube, Dnieper, and Don rivers, which drain almost one-third of the entire land area of continental Europe (Bakan and Büyükgüngör, 2000). A permanent feature is an upper-layer circulation driving the Rim Current, encircling the entire Black Sea and forming a large-scale cyclonic gyre (Korotaev *et al.,* 2003). This circulation induces a rise of sea level toward the coast, where velocities increase and conversely sea level decreases in the deeper margins of the Black Sea (Kubryakov and Stanichnyi, 2013). The amplitude of sea-level variation in space depends on seasonal influences, ranging from 25 to 40 cm (Korotaev *et al.,* 2003). Volkov and Landerer (2015) note that nonseasonal sea-level time series in the Black and Aegean seas (eastern Mediterranean) are significantly correlated, with the Black Sea, lagging by around 1 month.

Baltic Sea

Another semienclosed waterbody, The Baltic Sea is approximately 350,000 km^2 and is connected to the North Sea through the Kattegat and via the three Danish Straits (Øresund, Great Belt, and Little Belt) between Sweden and Denmark. The Gulf of Bothnia defines the northernmost extent the Baltic Sea, whilst the Gulf of Finland defines the easternmost extremity, extending all the way to Saint Petersburg, Russia. Based on the limited exchange with the open ocean, the Baltic Sea is virtually tideless but receives considerable freshwater inflows from more than 200 river systems (Leithe-Eriksen, 1992). The mean depth of the Baltic is around 50 m; however, the Gulfs of Bothnia and the central Baltic can be up to 500 m deep (Leppäranta and Myrberg, 2009). Ice typically covers the sea in winter months in the Gulfs of Bothnia, Finland, and Riga and in sheltered bays and lagoons (Kullenberg, 1981).

Whilst these waterbodies exhibit quite different physical characteristics, the associated land masses around Europe embody distinctive vertical land motions that are embedded within relative sea level records recorded at tide gauges. The most prominent of these are the high rates of postglacial rebound experienced within the Fennoscandian region of northern Europe (comprising Sweden, Finland, Norway, and parts of Russia), which are among the highest rates globally predicted by the ICE-6G (VM5a) model (Argus *et al.,* 2014; Peltier, Argus, and Drummond, 2015). Land uplift rates around the Baltic Sea margins range from 0 in the south to 9 mm/y in the north (Leppäranta and Myrberg, 2009). Elsewhere across Europe, areas are known to be subsiding, such as the eastern margins of the Black Sea and around the southern English and the Dutch and German coastlines (Bungenstock and Schäfer, 2009; Minshull *et al*., 2005; Shennan and Woodworth, 1992; Wahl *et al*., 2013). The Mediterranean Sea and Black Sea regions exhibit a complex range of concomitant land movement processes, including glacial isostatic adjustment; subsidence due to sediment compaction in key river delta areas such as the Po, Rhône, Ebro, and Danube (Ericson *et al.,* 2006; Panin and Jipa, 2002); and tectonic processes whereby collisions between the African, Eurasian, and Arabic plates have produced very complex tectonic regimes of microplates that are far from resolved, especially with respect to vertical motions (Garcia *et al.,* 2007).

METHODS

The methodology below follows the procedures espoused in Watson (2016c) that have been applied to the longest time series records available for Europe, which meet the msltrend package admissibility protocols (described further in the following “Data” section). In summary, there are four key steps to the analysis.

Step 1: Gap Filling

To perform singular spectrum analysis (SSA), the time series must be complete. Numerous methods are available for gap-filling time series data; however, for ocean water level records it is recommended to fill the gaps using SSA and recurrent forecasts from complete parts of the record (Golyandina and Osipov, 2007). Iterative gap filling using SSA (Kondrashov and Ghil, 2006) has been utilised to reconstruct the gap from the combination of SSA components in which the peak spectral frequency is ≤ 0.2 (alternatively, corresponding to peak periods ≥ 5 y). By doing so, the principal spectral structures evident in the complete parts of the record can be used to forecast with greater precision across the data gap.

The msltrend package places constraints on the amount and type of gaps within the time series. Douglas (1992) noted the importance of gaps in records because of the presence of low-frequency sea-level variations. For gap-filling procedures to maintain the integrity of records and not themselves unduly affect trend determination, the total data gaps and maximum continuous data gap are limited to 15% and 5%, respectively, of the length of the time series. All gap-filled sections have been visually inspected to provide a sanity check on the synthetic data sections generated.

Step 2: Isolating Trend Using SSA

Once gap filling has been completed, msltrend decomposes the time series using 1D-SSA with a window (or embedding dimension) of half the time series length to optimise the detail of the decomposition and improve the separability of key signals (Golyandina and Zhigljavsky, 2013). The trend component(s) from the SSA decomposition are then isolated using spectral thresholding techniques to capture and reconstruct only components in which 75% of the contribution for each component is confined within the low frequency band (0–0.01). These specific limits have been established from inspection of the decomposition of the 50 longest records within the data repository of the PSMSL. The grouping of relevant components are automatically detected and reconstructed within msltrend to estimate relative mean sea level.

Step 3: Estimating Real-Time Velocity and Acceleration

A cubic smoothing spline is then fitted to the trend determined in step 2 to estimate the real-time (or instantaneous) velocities and accelerations corresponding to each data point in the original time series. As the trend by definition is comparatively smooth, the fitted smoothing spline has been limited to one degree of freedom for every eight data points. The coefficient of determination (R^2) between the SSA-derived trend and the fitted cubic smoothing spline for all records analysed exceeds 0.99, representing a near mathematically perfect model fit.

The instantaneous velocity and accelerations can be readily estimated from the first and second derivatives of the fitted smoothing spline, respectively, corresponding to the original time steps in the series. However, care is required in fitting smoothing splines and deriving second derivatives near the end of the time series, because the knots at the end of a fitted cubic smoothing spline are fixed in order to be differentiable, resulting in a second derivative at the ends that must converge to zero. For this reason, the first and last three derived acceleration points on the time series will likely have reduced accuracy and are not included in any analysis.

Step 4: Calculation of Errors

Errors in estimating the trend and associated instantaneous velocity and accelerations have been determined using block bootstrapping techniques with 10,000 iterations. This process initially involves fitting an autoregressive time series model to remove the serial correlation in the residuals between the SSA-derived trend and the gap-filled time series (Foster and Brown, 2015).

The uncorrelated residuals are then tested to identify change points in the statistical variance along the time series. Where a change point in the variance is detected, the recommended procedure involves block bootstrapping of uncorrelated residuals quarantined between identified variance change points and then adding the sections to the SSA-derived trend before running steps 2 and 3 some 10,000 times. The standard deviations are then readily calculated for the trend, as well as associated velocity and accelerations from which to directly derive confidence intervals. All error margins in the paper have been estimated at the 95% confidence level (unless specified otherwise).

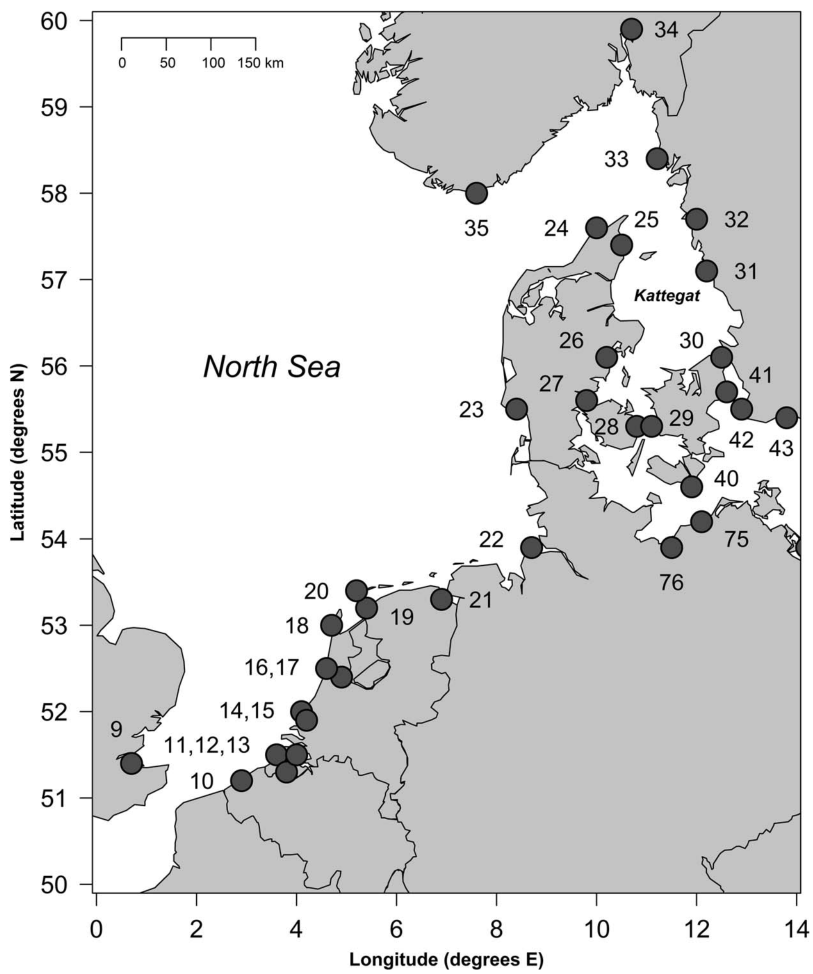

Figure 2. North Sea tide gauge records analysed for this study. Refer to Figure 1 inset A and Table 1 for further details.

Mean Sea-Level Data

The msltrend package was specifically developed for application to annual average time series data available from the PSMSL. Data records are required to have a minimum length of 80 years to more robustly decompose the time series and improve the accuracy of isolating the trend from the range of complex time-varying amplitude influences, including the quasi 60-year oscillation identified in all oceanic basins of the world (Chambers, Merrifield, and Nerem, 2012). Only revised local reference datasets from the PSMSL have been used because they are commensurate with quality control procedures and complete tide gauge datum histories provided by the supplying national authority (PSMSL, 2016).

Within the study area (Figure 1), some 83 annual average time series records are available for analysis that meet the length and data gap admissibility protocols of the msltrend package. Within these records, the spatial density is highest along the northern and central European mainland bordering the North Sea and for margins around the Baltic Sea, contrasting sharply with the scarcity of comparable records within the Mediterranean and Black seas. Records used in this study comprise 8505 station years from the PSMSL plus a further 2436 station years added through the extensive data archaeology work of Hogarth (2014). The work of Hogarth (2014) extends tide gauge time series from the PSMSL using historical documents and PSMSL ancillary data and by developing additional composite time series using near-neighbour tide gauges (Watson, 2016c). A total of 54 station records used in this study have been extended by Hogarth (2014), with only the complete portions of these extended time series used. Furthermore, only records finishing within the last decade (post 2006) have been considered, because the focus of the study is to reconcile recent temporal changes in mean sea level with the historical record available.

All data records used have notionally been assigned a "Station ID" (Table 1) based on differentiating key European coastlines, including: (1) North Atlantic commencing in the south at Lagos, Portugal (ID = 1), heading north around the British Isles, along the North, Norwegian, and Barents seas to Polyarniy, Russian Federation (ID = 39) (Figures 1 and 2); (2) Baltic Sea beyond the entrance at the Great Belt commencing at Gedser, Denmark (ID = 40), moving in a clockwise direction

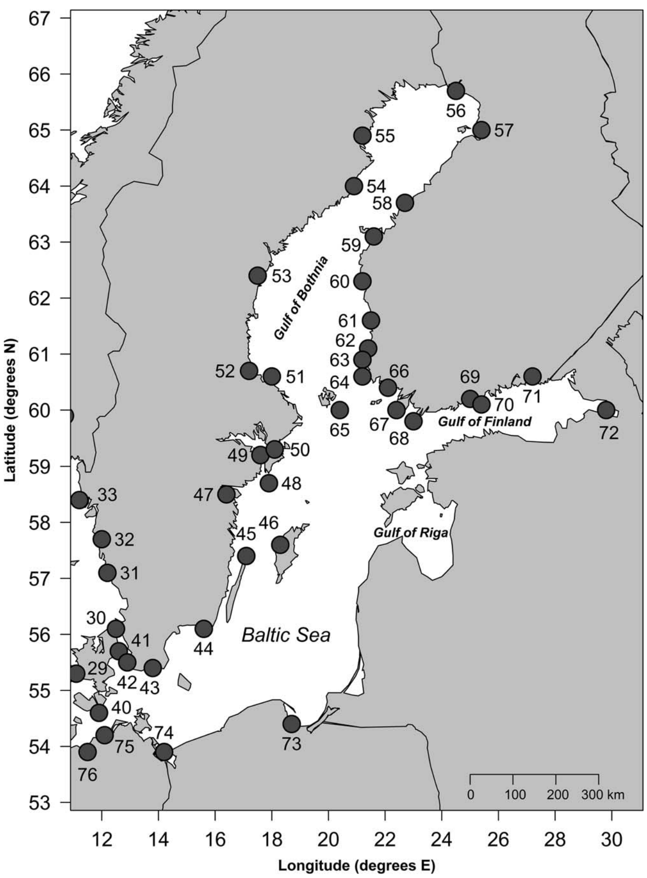

Figure 3. Baltic Sea tide gauge records analysed for this study. Refer Figure 1 inset B and Table 1 for further details.

around the Gulf of Bothnia, Gulf of Finland, and Gulf of Riga to Wismar, Germany (ID = 76) (Figure 3); and (3) Mediterranean and Black seas beyond the Strait of Gibraltar commencing at Alicante, Spain (ID = 77), moving in a clockwise direction around the Balearic, Tyrrhenian, Ionian, Adriatic, and Aegean seas, to Poti, Georgia (ID = 83), on the eastern foreshore of the Black Sea (Figure 1).

By graphically representing characteristics associated with records based on the Station ID, spatially dominant patterns are more readily apparent.

Estimates of Geocentric Mean Sea Level

Système d'Observation du Niveau des Eaux Littorales (SONEL) vertical land movement data have been used to correct relative rates of sea-level rise to estimate geocentric rates. Specifically, the relative rate of mean sea level applied is the last (or most recent) velocity determined from step 3 above. The additional assessment of geocentric rates of mean sea level across Europe permit valuable and direct comparison against the contemporary rate of global mean sea level estimated from satellite altimetry (CU Sea Level Research Group, 2016). SONEL serves as the Global Navigation Satellite System (GNSS) data assembly centre for the Global Sea Level Observing System. The SONEL recently undertook the reanalysis of 19 years of Global Positioning System (GPS) data from 1995 to 2014, providing the updated ULR6a solution for vertical land velocities for GNSS sites within approximately 15 km of long tide gauge records used in this study (Santamaría-Gómez *et al.*, 2012; SONEL, 2016). In situations where several alternative SONEL stations were available to choose from, selection was based upon the GPS site located closest to the tide gauge, where the GPS antenna is still active (Table 1). In total, 30 SONEL stations with updated ULR6a solutions were available for application within the study area.

Statistical Significance Testing

An important aspect of the analysis contained herein is to determine whether more recent peak velocities and accelerations associated with mean sea level are statistically different (higher) than rates measured elsewhere over the course of the historical record. To do this, the statistical significance tests advised by Wolfe and Hanley (2002) have been applied at the 95% confidence level.

RESULTS

Figure 4 provides an example output from the analysis of the four longest records available within the study area (Amsterdam, Netherlands, 246 y; Stockholm, Sweden, 214 y; Brest, France, 208 y; and Swinoujscie, Poland, 202 y), reflective of the broader regional temporal signatures of velocity and accelerations in relative mean sea level. It is clear that these velocities and accelerations are varying over time. It is also evident from these long records that relative velocity is steadily increasing over time, peaking at or near the recent end of the time series record, driven by low and continually changing rates of acceleration. For each of the long records depicted in Figure 4, the acceleration is predominantly confined to a narrow band within ± 0.05 mm/y^2 and not statistically different from zero at the 95% confidence level for most of the records, despite evidence that relative velocities are continuing to increase. The complete analysis of all the records in this manner provides the means to inspect spatiotemporal patterns in greater detail than previously available.

Figure 5 provides a breakdown of the peak velocities and accelerations for each record and the time they occur. It is relevant to consider these charts simultaneously because velocity and acceleration are intrinsically linked as kinematic properties. For example, acceleration is required to increase velocity and conversely negative acceleration (or deceleration) is required to reduce velocity. From inspection of Figure 5, a range of key observations are apparent.

The spatial signature of peak relative velocity is strongly reflective of the signatures of vertical land movements within the study area. Those areas experiencing high rates of postglacial rebound are clearly evident moving northward around the Baltic Sea margins, and peak relative velocities are less than –4 mm/y. Conversely, only 19 stations measure a peak relative velocity throughout the historical record exceeding 2 mm/y (Table 2). Principally these high rates correspond with areas that exhibit known subsidence (eastern Black Sea, southern English, Dutch, and German coastlines). The primary and secondary velocity peaks measured across all European records are quite similar in magnitude. Some 52 of the 83

Table 1. *Summary of data used in this study.*

Tide Gauge Data							GNSS (GPS) Data[c]			
Station ID[a]	Location	PSMSL ID	Year Start	Year End	Length (y)	Gaps (y)	SONEL Station	Length (y)	Distance to Tide Gauge (m)	VLM (mm/y)
North Atlantic Ocean (including North Sea, Norwegian Sea, and Barents Sea)										
1	Lagos[b]	162	1909	2012	104	14	LAGO	13.72	134	−0.52 ± 0.15
2	Cascais[b]	52	1882	2012	131	14	CASC	15.63	275	−0.08 ± 0.18
3	Leixoes[b]	791	1928	2008	81	12	GAIA	NA	12,677	
4	Saint-Jean-de-Luz[b]	469	1889	2013	125	15	SCOA	8.01	2	−2.70 ± 0.28
5	Brest	1	1807	2014	208	23	BRST	15.16	293	−0.02 ± 0.11
6	Newlyn	202	1916	2014	99	2	NEWL	15.24	5	−0.21 ± 0.13
7	Aberdeen[b]	21	1862	2014	153	11	ABER	15.28	1	0.90 ± 0.22
8	North Shields[b]	95	1895	2014	120	2	NSLG	3.94	495	1.37 ± 0.67
9	Sheerness[b]	3	1870	2008	139	1	SHEE	16.57	2	1.09 ± 0.20
10	Oostende[b]	413	1927	2012	86	6	OOST	10.65	966	−0.35 ± 0.28
11	Vlissingen	20	1862	2014	153	—	VLIS	7.1	2	0.28 ± 0.51
12	Terneuzen[b]	—	1862	2008	147	—	—	—	—	—
13	Hansweert[b]	—	1862	2008	147	—	—	—	—	—
14	Hoek van Holland	22	1864	2014	151	—	—	—	—	—
15	Maassluis	9	1848	2014	167	—	—	—	—	—
16	Amsterdam[b]	—	1766	2011	246	—	—	—	—	—
17	IJmuiden[b]	32	1872	2014	143	—	IJMU	9	2	−0.53 ± 0.34
18	Den Helder[b]	23	1832	2014	183	—	—	—	—	—
19	Harlingen[b]	25	1865	2014	150	—	—	—	—	—
20	West-Terschelling	236	1921	2014	94	—	TERS	17.16	10	−0.20 ± 0.22
21	Delfzijl[b]	24	1827	2014	188	1	—	—	—	—
22	Cuxhaven[b]	7	1843	2013	171	—	TGCU	5.02	1	0.01 ± 0.86
23	Esbjerg	80	1889	2012	124	3	ESBH	9.13	5	−1.18 ± 0.48
24	Hirtshals	89	1892	2012	121	10	HIRS	9.13	512	2.75 ± 0.45
25	Frederikshavn	91	1894	2012	119	8	—	—	—	—
26	Aarhus	76	1889	2012	124	8	—	—	—	—
27	Fredericia	81	1890	2012	123	3	—	—	—	—
28	Slipshavn	98	1896	2012	117	10	—	—	—	—
29	Korsor	113	1897	2012	116	6	—	—	—	—
30	Hornbæk[b]	119	1891	2013	123	4	—	—	—	—
31	Varberg[b]	73	1887	2012	126	—	—	—	—	—
32	Goteborg-Ringon[b]	2133	1887	2012	126	1	—	—	—	—
33	Smogen[b]	179	1895	2014	120	—	—	—	—	—
34	Oslo[b]	62	1914	2014	101	—	OSLS	13.16	28,041	5.31 ± 1.12
35	Tregde	302	1928	2014	87	5	TGDE	9.78	5	1.64 ± 0.41
36	Bergen[b]	58	1915	2014	100	4	—	—	—	—
37	Heimsjo	313	1928	2014	87	11	—	—	—	—
38	Kabelvag[b]	45	1928	2014	87	4	—	—	—	—
39	Polyarniy[b]	2027	1926	2012	87	6	—	—	—	—
Baltic Sea Region										
40	Gedser[b]	120	1882	2012	131	2	GESR	9.17	200	0.61 ± 0.66
41	Kbenhavn	82	1889	2012	124	4	BUDP	10.99	8817	1.99 ± 0.51
42	Klagshamn	330	1930	2014	85	—	—	—	—	—
43	Ystad[b]	72	1887	2012	126	—	—	—	—	—
44	Kungsholmsfort	70	1887	2014	128	—	—	—	—	—
45	Olands Norra Udde[b]	69	1887	2014	128	—	—	—	—	—
46	Visby	2105	1916	2014	99	1	VIS0	14.83	5195	3.31 ± 0.56
47	Mem[b]	75	1864	2013	150	—	—	—	—	—
48	Landsort[b]	68	1887	2012	127	—	—	—	—	—
49	Nedre Sodertalje[b]	31	1869	2014	146	—	—	—	—	—
50	Stockholm[b]	78	1801	2014	214	—	—	—	—	—
51	Bjorn[b]	90	1892	2013	122	—	—	—	—	—
52	Nedre Gavle[b]	99	1896	2013	118	—	MAR6	14.83	11,000	7.86 ± 0.65
53	Draghallan[b]	122	1898	2013	116	1	SUN6	NA	16,017	
54	Ratan	88	1892	2014	123	1	—	—	—	—
55	Furuogrund[b]	203	1892	2014	123	2	SKEO	8.99	9530	10.43 ± 0.20
56	Kemi	229	1920	2014	95	9	—	—	—	—
57	Oulu	79	1889	2014	126	18	—	—	—	—
58	Pietarsaari[b]	194	1889	2014	126	5	—	—	—	—
59	Vaasa[b]	57	1867	2014	148	11	VAAS	14.83	20,000	9.13 ± 0.13
60	Kaskinen	285	1927	2014	88	6	—	—	—	—
61	Mantyluoto[b]	172	1889	2014	126	4	—	—	—	—
62	Rauma	376	1933	2014	82	2	—	—	—	—
63	Lyokki[b]	16	1858	2013	156	1	—	—	—	—
64	Lypyrtti[b]	17	1858	2013	156	1	—	—	—	—

Table 1. Continued.

		Tide Gauge Data					GNSS (GPS) Data[c]			
Station ID[a]	Location	PSMSL ID	Year Start	Year End	Length (y)	Gaps (y)	SONEL Station	Length (y)	Distance to Tide Gauge (m)	VLM (mm/y)
65	Foglo[b]	249	1866	2014	149	8	—	—	—	—
66	Turku	239	1922	2014	93	3	—	—	—	—
67	Jungfrusund[b]	18	1858	2011	154	17	—	—	—	—
68	Hanko[b]	71	1866	2014	149	17	—	—	—	—
69	Helsinki	14	1879	2014	136	—	METS	18.99	31,729	4.48 ± 0.84
70	Soderskar[b]	29	1866	2014	149	—	—	—	—	—
71	Hamina[b]	315	1889	2014	126	4	—	—	—	—
72	Kronstadt[b]	—	1835	2011	177	—	—	—	—	—
73	Gdansk[b]	64	1886	2011	126	5	—	—	—	—
74	Swinoujscie[b]	2	1811	2012	202	2	—	—	—	—
75	Warnemunde[b]	11	1855	2014	160	1	WARN	10.87	126	0.65 ± 0.59
76	Wismar	8	1849	2014	166	1	—	—	—	—
Mediterranean Sea (including Black Sea)										
77	Alicante[b]	208	1874	2010	137	11	ALAC	14.4	1	0.33 ± 0.19
78	Marseille[b]	61	1885	2014	130	1	MARS	15.45	5	−0.24 ± 0.18
79	Genova[b]	59	1884	2013	130	16	GENO	15.43	1000	−0.22 ± 0.27
80	Venezia[b]	168	1872	2012	141	7	VEN1	4.18	5825	−1.21 ± 0.67
81	Trieste[b]	154	1875	2015	141	2	TRIE	10.89	6707	0.30 ± 0.27
82	Tuapse	215	1917	2014	98	2	TUAP	NA	95	—
83	Poti	41	1874	2013	140	9	—	—	—	—

Abbreviations: VLM = vertical land movements; NA = not available
[a] The "Station ID" is a local referencing protocol used throughout this study, particularly the graphical outputs.
[b] Extended data sets advised in Hogarth (2014) have been used for this study.
[c] All GPS data kindly provided by SONEL using updated ULR6a solutions (Santamaría-Gómez *et al*., 2012) with 1σ error estimates advised.

records (63%) have the peak relative velocity occurring on or after 2000, although within this figure there are some interesting spatial features. In particular, this figure rises to 80% of the stations in the semienclosed seas (Baltic, Mediterranean, and Black seas), in contrast to only 44% of the stations positioned along the North Atlantic coastline. Some 10 of these peaks coincide with the most recent data point in the time series (Brest, France [ID = 5]; Bergen, Norway [ID = 36]; Heimsjo, Norway [ID = 37]; Mem, Sweden [ID = 47]; Swinoujscie, Poland [ID = 74]; Alicante, Spain [ID = 77]; Marseille, France [ID = 78]; Genova, Italy [ID = 79]; Trieste, Italy [ID = 81]; and Tuapse, Russian Federation [ID = 82]).

Table 2. Summary of maximum relative velocity >2 mm/y.

Station ID[a]	Location	Peak Relative Velocity (mm/y)	Year
83	Poti	7.88	1988
13	Hansweert	4.31	1981
73	Gdansk	3.47	2004
82	Tuapse	3.45	2014
12	Terneuzen	3.42	1949
80	Venezia	2.82	1901
14	Hoek van Holland	2.74	1864
4	Saint-Jean-de-Luz	2.55	1910
16	Amsterdam	2.40	2000
22	Cuxhaven	2.36	1865
9	Sheerness	2.34	2000
17	Ijmuiden	2.34	1993
11	Vlissingen	2.26	1997
6	Newlyn	2.25	1916
10	Oostende	2.24	2000
1	Lagos	2.20	1909
8	North Shields	2.08	1909
78	Marseille	2.05	2014
21	Delfzijl	2.04	1995

[a] Refer to Table 1 for further station details.

Mean maximum acceleration measured across all records is approximately 0.074 ± 0.042 mm/y^2 (1σ), with no particular spatial patterns evident.

There is, however, strong spatial coherence around the timing of the primary and secondary peaks in mean sea level acceleration (middle right panel), with nearly 34% of the peak acceleration focused within a band between 1994 and 2000. Other bands of acceleration are clearly evident centred around 1940 and 1976.

Most significantly, from an analysis of the peak velocities and accelerations for all records considered within the study area, only five peak velocities (Hornbæk, Denmark [ID = 30]; Smögen, Sweden [ID = 33]; Kbenhavn, Denmark [ID = 41]; Furuögrund, Sweden [ID = 55]; and Genova, Italy [ID = 79]) and three peak accelerations (Vlissingen, Netherlands [ID = 11]; IJmuiden, Netherlands [ID = 17]; and Marseille, France [ID = 78]) are statistically different (or higher) than other peaks observed elsewhere over the historical record (95% confidence level). Of these eight statistically significant peaks, all except the peak accelerations measured at Vlissingen and Ijmuiden occur after 1990.

Figure 6 provides an assessment of the extent and temporal distribution of positive acceleration in all records that is statistically different from zero. Such analyses provide an alternative form of assessment for investigating subtleties of acceleration when the metrics are comparatively low. A mere 7.4% of the 10,941 station years of records available exhibit a positive acceleration different from zero at the 95% confidence level. However, there is some evidence of a more sustained period of positive acceleration between ≈1880 and 1910 from the longer records available for the southern portion of the North Atlantic coastline. Elsewhere the temporal signatures mirror the peak accelerations discussed previously concerning

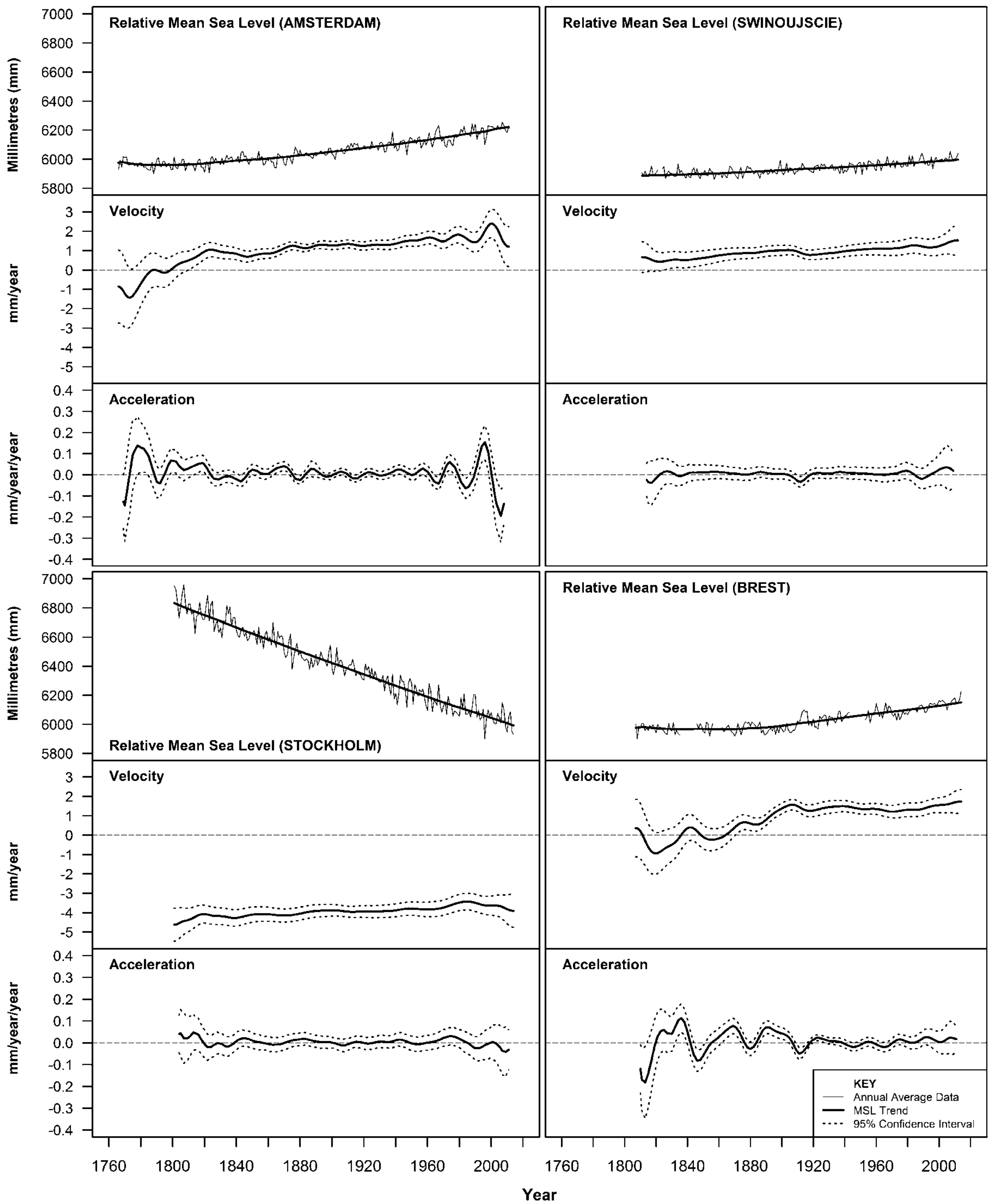

Figure 4. Temporal characteristics of mean sea level for the longest records within the study area (Amsterdam, Netherlands; Stockholm, Sweden; Brest, France; and Swinoujscie, Poland). Each site is depicted by a three-panel plot of mean sea level, velocity, and acceleration. The respective scales are identical for all stations for direct comparative purposes.

Figure 5. Results displayed in Figure 6 also highlight a difference within the Baltic Sea compared with the rest of the study area. Specifically, only 2.6% of station years exhibit a positive acceleration different from zero, with some 54% of the Baltic records indicating no positive acceleration throughout the time series (95% CI).

Figure 7 provides an appraisal of the current rate of geocentric sea-level rise across the tide gauge network by

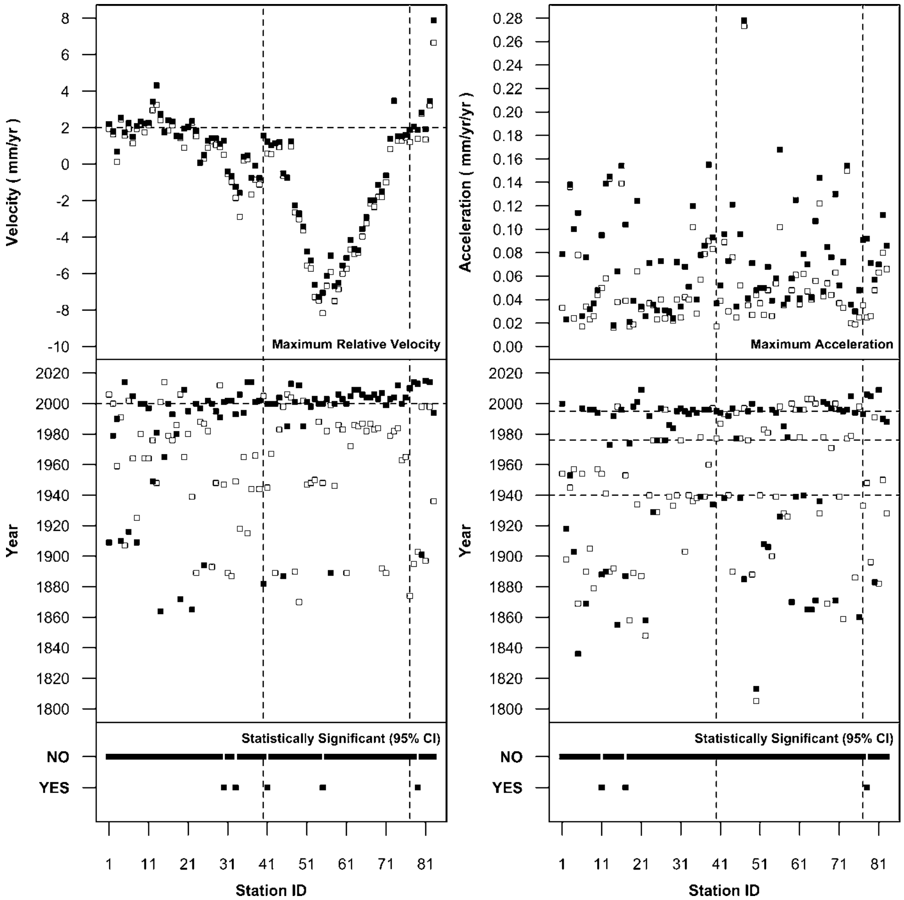

Figure 5. Peak estimates of velocity and acceleration for all stations. Peak metrics are denoted as filled boxes, whilst secondary peaks are denoted by clear boxes. The centre panels indicate the year in which the respective peaks occurred. A vertical dashed line corresponding to station 40 (Gedser, Denmark) and station 77 (Alicante, Spain) denote the commencement of the Baltic Sea stations and Mediterranean Sea and Black Sea stations, respectively. Horizontal lines are provided as visual markers correlating to relevant discussions in the text. The bottom panel provides an indication as to whether the peak metric is statistically different (in this case higher) than all others in the context of the historical record at the 95% confidence level based on the significance testing protocol advised in Wolfe and Hanley (2002). Station ID references are summarised in Table 1.

correcting the relative velocity at the recent end of the record with GPS-derived vertical land movement rates from SONEL (Table 1), noting that only 30 records (or 36%) have an associated SONEL station available with updated ULR6a solutions (Santamaría-Gómez et al., 2012; SONEL, 2016). A number of key features are evident from this graphical analysis, including no evident spatial trend across Europe from the current geocentric velocities. Furthermore, none of the geocentric velocities determined exceed the global average of 3.4 ± 0.4 mm/y (CU Sea Level Research Group, 2016; Nerem *et al.*, 2010) at the 95% confidence level. Ten stations, though, are lower than the global average (95% CI), of which eight are located along the North Atlantic coastline between Lagos, Portugal (ID = 1), and Esbjerg, Denmark (ID = 23).

The bottom panel of Figure 7, although highlighting no particular spatial pattern across Europe, indicates that only 25 of 83 stations (or 30%) exhibit a current velocity exceeded by <10% of the historical record. For these stations, this indicates the latter portions of these records are within the upper bracket of velocities recorded over the historical record, providing tangible (albeit limited) evidence of recent acceleration in mean sea level across the European region.

DISCUSSION

Watson (2016b,c) notes that although extensive research has been undertaken into sea-level rise, considerable conjecture and scientific debate remain about the temporal changes in mean sea level and the climatic and associated physical forcings responsible for them. One of the reasons for this is that ocean water level time series data from tide gauge stations are a complex amalgam of key physical contributory factors that include: (1) land movement at the tide gauge site; (2) dynamic influences of largely oceanographic, atmospheric, or gravitational origins operating on differing temporal and spatial scales; and (3) a low-amplitude signal of mean sea-level rise driven by climate change influences (principally, melting of snow and ice reserves bounded above sea level [directly adding water] and thermal expansion of the ocean water mass).

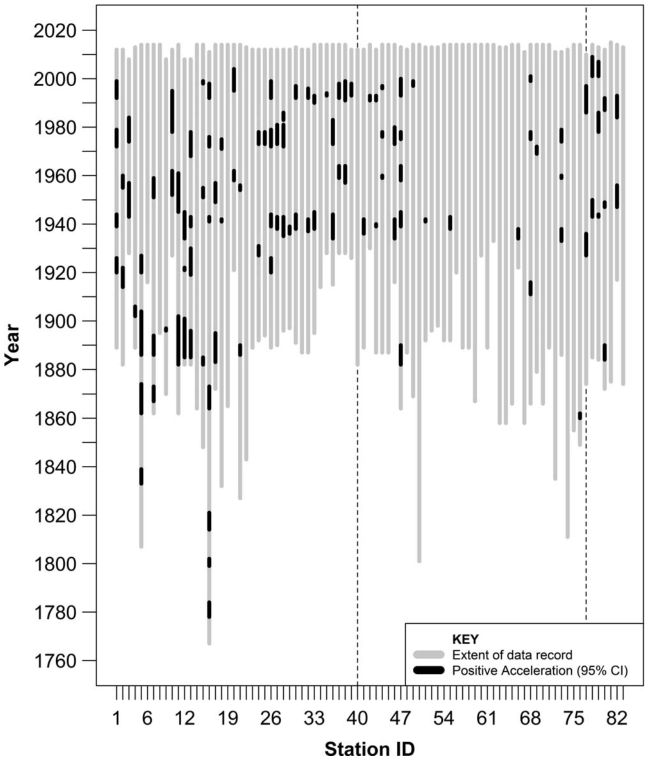

Figure 6. Summary of periods of positive acceleration (95% confidence interval).

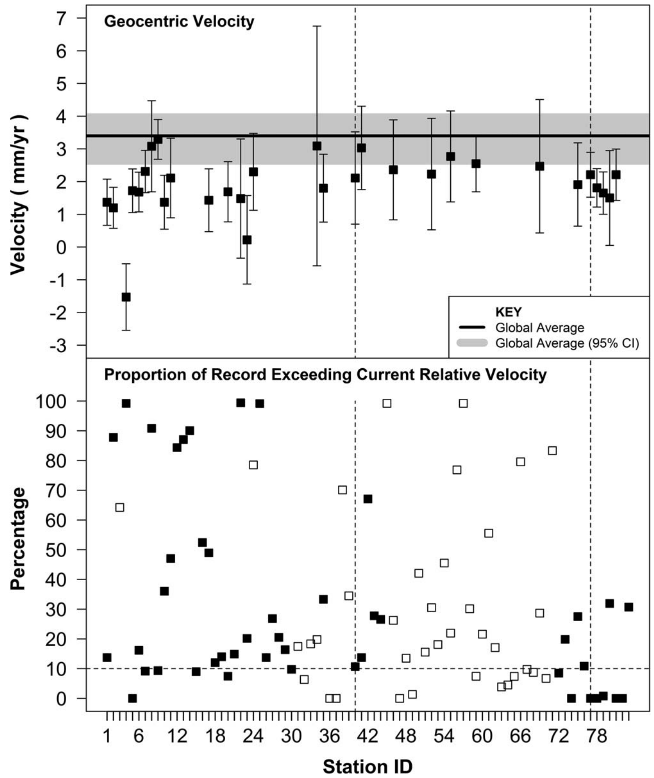

Figure 7. Current estimates of geocentric rate of sea-level rise (95% confidence interval). "Current" refers to the last date in the respective data time series. Estimates based on real-time relative velocity derived from msltrend decomposition corrected by vertical land movement velocities provided by SONEL. The vertical dashed lines demarcate the three respective spatial subregions analysed (North Atlantic Ocean, Baltic Sea, and Mediterranean Sea; refer to Table 1). Clear boxes in the bottom panel represent stations in which relative sea-level fall is evident over the course of the record. Data sources and station ID references are summarised in Table 1.

Specifically within the European context, factors 1 and 2 are particularly complex. The study area encompasses sites ranging from those that exhibit high rates of vertical land motion from postglacial rebound (*e.g.,* Baltic Sea) to areas where significant ongoing subsidence is prevalent (*e.g.,* eastern margins of the Black Sea). Additionally, the semienclosed margins of the Black, Mediterranean, and Baltic seas drain annual continental water discharges from large tracts of Europe.

Deshayes and Frankignoul (2008) note that the North Atlantic Ocean is a key element of Earth's climate. In particular, the cyclonic circulation at depth along the boundaries, the deep western boundary current, is the deep limb of the Atlantic meridional overturning circulation (AMOC) that contributes substantially to the energy balance of the earth. The state of the North Atlantic Oscillation (NAO) imposes a strong constraint on the circulation of the North Atlantic (Getzlaff *et al.,* 2005) and is considered to be a singular major atmospheric, basin-scale pattern that affects sea level around Europe and further afield (Tsimplis *et al.,* 2006; Wakelin *et al.,* 2003; Woolf, Shaw, and Tsimplis, 2003).

In addition to the afore-mentioned studies, numerous published works have been dedicated to examining linkages between dominant NAO drivers and sea-level anomalies throughout the study area (*e.g.,* Calafat, Chambers, and Tsimplis, 2012; Dangendorf *et al.*, 2012; Gomis *et al.,* 2006, 2008; Jevrejeva, *et al.,* 2005; Lehmann, Getzlaff, and Harla, 2011; Tsimplis *et al.,* 2008; Tsimplis and Shaw, 2008; Vigo, Garcia, and Chao, 2005).

Tsimplis and Shaw (2008) note the NAO influence causes an anticorrelation between northern and southern European sea level, whilst Yan, Tsimplis, and Woolf (2004) observed a linear relationship between sea-level anomalies and the winter-averaged NAO index in NW Europe ranging from about −100 to +200 mm per NAO unit (Wakelin *et al.,* 2003; Woolf, Shaw, and Tsimplis, 2003). The NAO remains the most significant dynamic influence (factor 2 above) embedded within European ocean water level time series.

Improving estimates of relative mean sea level (factor 3 above) and associated kinematic properties (velocity, acceleration), rests largely with improved isolation of these dynamic contaminating influences from the time series. These influences persist on interannual to decadal (and longer) timescales resulting ostensibly from winds driven by climate modes (Qiu and Chen, 2012; Sturges and Douglas, 2011) and are often orders of magnitude larger in scale than the low-amplitude signal of mean sea-level rise, which is the key artefact of interest (Watson, 2016c). The necessity to remove these influences from the data to enhance acceleration estimates is well noted in the literature (*e.g.,* Calafat and Chambers, 2013; Calafat, Chambers, and Tsimplis, 2012; Chambers, Merrifield, and Nerem, 2012; Dangendorf *et al*., 2014; Douglas, 1992; Haigh *et al*., 2014).

The NAO was one of the key dynamic features embedded within the synthetic data set (Watson, 2015) used to test time series analysis techniques for their utility in isolating relative mean sea level from conventional ocean water level data sets with improved accuracy (Watson, 2016a). From this testing, SSA (which underpins the msltrend package used to decompose records in this study) proved an optimal technique to separate out these complex oscillatory signals with time-varying amplitudes and noise from the low-amplitude and low-frequency signal of mean sea-level rising over time. In particular, the estimation of mean sea level via selection of "trend-like" components in which a contribution threshold $\geq$75% is contained within frequency bins $\leq$0.01 (refer to "Methods," step 2) provides a necessary assurance that these dynamic contaminating influences are removed.

The detailed analysis undertaken highlights that velocity time series associated with relative mean sea level at each site are distinctly nonlinear, in turn reflective of associated acceleration continually varying over time. With relatively small kinematic properties evident over the course of the lengthy records available (Figure 4), different diagnostic approaches are proving necessary to infer an acceleration in mean sea level records or to detect change points in records that might be reflective of an altered climate-related forcing. The relative mean sea-level velocity and acceleration time series enable subtle changes to be more readily or intuitively detected, moving beyond the encumbrances and inherent limitations of the overly used linear regression and quadratic techniques to estimate velocity and acceleration, respectively (refer to "Discussion" in Watson, 2016c).

Reconciling Historical and Future Projected Mean Sea Level Accelerations

As indicated above, the scale of velocities and accelerations measured within this study (*e.g.,* Figure 4) are relatively small, particularly when compared with those associated with forecasts from physics-based and climate models over the course of the 21st century and beyond (IPCC, 2013). Under various forecast scenarios, the current rate of global averaged sea-level rise of 3.4 $\pm$ 0.4 mm/y (CU Sea Level Research Group, 2016; Nerem *et al.,* 2010) is expected to increase to rates of the order of 10–20 mm/y by 2100 (Watson, 2016a).

Figure 8 provides a visual comparative analysis of how the velocity and acceleration time series might change at Cuxhaven, Germany, and Kronstadt, Russian Federation, based on a relative mean sea-level rise of 800 mm from present to 2100. Under such a scenario, which assumes simple equations of motion and uniform acceleration, the necessary and significant changes in velocities and accelerations compared with those measured over the historical record, are likely to be readily apparent well within the next 20 years. For example, accelerations at both stations will, under such a scenario, have to rise to $\approx$0.18 mm/y^2 within the next 10 years and be sustained to 2100. By contrast, only one European record (Mem, Sweden) has experienced a measured acceleration of this order from the 10,941 station years analysed (Figure 5), and from all of these records, a mere 7.4% exhibit a positive acceleration different from zero at the 95% confidence level (Figure 6).

One should caution that these forecasts are highly idealistic and preliminary. They are advised to provide a sense of perspective regarding the timing of necessary changes to the kinematic properties of mean sea level at these locations, in order to give effect to such projections. It is recognised that the atmosphere is regarded as having a very short memory, whereas the oceans, because of their enormous thermal inertia, provide much longer memory for climate variations (Dangendorf *et al.,* 2015; Marcos *et al.,* 2016; Trenberth and Hurrell, 1994). This inertia and long-term memory relate to the ability and time for the ocean to store and transport heat and temperature anomalies throughout the water mass to great depth (Goosse *et al*., 2004; Goosse and Renssen, 2005). Whilst these facets are built into coupled ocean–atmosphere general circulation models to study the characteristics of the large-scale ocean circulation and its climatic effects, the trajectory of the oceanic response remains uncertain, with potential lags not yet fully understood.

From this perspective it is imperative to appreciate the importance of ongoing efforts to identify, with improved accuracy, critical change points in the long time series of mean sea-level records available. Whilst the techniques espoused in this paper represent a concerted effort to test and specifically identify enhanced techniques to isolate mean sea level with improved temporal accuracy (Watson, 2015, 2016a,b,c) this work should be considered a staging point for ongoing improvements in such critical areas, in particular the identification of statistically robust change points in the record.

Selected Literature Concerning Mean Sea Level Acceleration around Europe

Woodworth (1990) remains one of the seminal papers in the literature concerning mean sea-level accelerations, focusing on the extensive network of European time series records. This work concluded that European tide gauge records since 1870 showed little evidence for significant accelerations, either positive or negative, in regional mean sea levels, with a weak deceleration observed on average. This study, however, based estimates of acceleration on simple quadratic coefficients, which (from a more contemporary understanding) have significant limitations (Watson, 2016c).

No comparable studies of this scale regarding mean sea level acceleration across Europe have been undertaken since Woodworth (1990), although considerable attention has been given to investigations on smaller scales, such as the North Sea (*e.g.,* Shennan and Woodworth, 1992; Wahl *et al*., 2013), English Channel, UK (*e.g.,* Haigh, Nicholls, and Wells, 2009), German Bight (*e.g.,* Wahl, Jensen, and Frank, 2010; Wahl *et al*., 2011), and Baltic Sea (*e.g.,* Donner *et al*., 2012; Spada, Olivieri, and Galassi, 2014).

Shennan and Woodworth (1992) analysed records from the U.K. and North Sea, developing a detrended "Regional Sea-Level Index," confirming the previous results of Woodworth

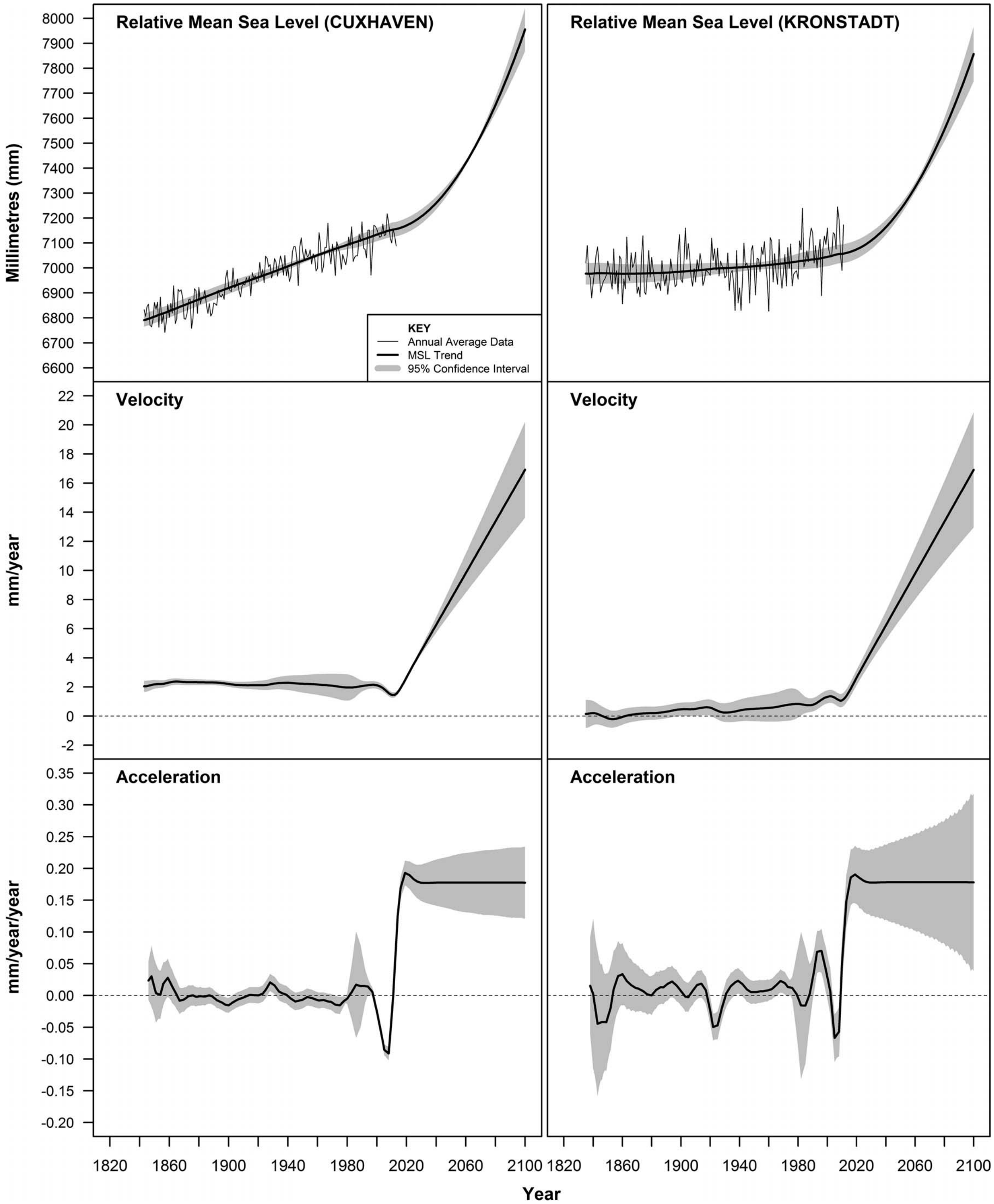

Figure 8. Indicative implications of projected sea-level rise of 800 mm at Cuxhaven, Germany, and Kronstadt, Russian Federation, from present to 2100. Projections are based on simple equations of motion with uniform acceleration. Error margins noted are 95% confidence levels.

(1990) with no evidence in the region for an acceleration of sea-level trends in recent decades (*i.e.* up to 1992).

Haigh, Nicholls, and Wells (2009) provide a detailed appraisal of available records around the English Channel. Acceleration in mean sea level was observed by considering overlapping 10, 25, and 50-year periods for the four longest and most complete records. The analysis concluded that recent high rates of change in mean sea level were not unusual compared with those that had occurred at other times in the 20th century, with no evidence as yet (at 2009) for any acceleration in sea-level rise over the 20th century around the English Channel.

Wahl *et al*. (2011) provides a detailed assessment of 13 tide gauge records covering the entire German North Sea coastline with particular consideration given to the investigation of nonlinear (acceleration) behaviour. One method involves the establishment of a "virtual" station time series smoothed using SSA (with an embedding dimension of 15 y) in combination with Monte Carlo autoregressive padding (used previously in Wahl, Jensen, and Frank, 2010) in a novel approach designed to limit the ubiquity of end effects associated with filtering of time series. Rates of change are then considered via first differences. This work concluded that an acceleration of sea-level rise commenced at the end of the 19th century with another distinct period of acceleration starting in the 1970s and intensifying from the 1990s, but the high rates of sea-level rise during this period are comparable to rates at other times during the last 166 years. Similar periods of key acceleration are confirmed in the current study, although Wahl *et al*. (2011) do not find evidence of acceleration around 1940 that is clearly evident in the current study and that of others (*e.g.,* Woodworth *et al.,* 2009). Of particular interest Wahl *et al*. (2011) also conclude recent (*i.e*. post-1990) rates of rise from nonlinear smoothing on the order of 4–6 mm/y for the southern part of the German Bight and 7–8 mm/y for the eastern part. Although the current study finds high recent (post-1990) rates of relative sea-level rise for records around the German Bight, the maximum rates determined are only on the order of ≈2 mm/y.

The discrepancy in the rates between the studies might, in part, rest with the comparatively narrow embedding dimension (or window length, L) of 15 years used for the SSA analysis in the Wahl *et al*. (2011) study. The selection of small window lengths risks suboptimal separability and potential mixing of signals, where the singular values of the decomposition are close. The smaller the embedding space, the shorter the length of the window over which the resolved components are calculated, and the less resolved is each component (Moore, Grinsted, and Jevrejeva, 2005). In effect, small SSA windows act like smoothing linear filters of width $2L-1$, thereby retaining contaminating power bands (albeit smoothed), as distinct from their isolation and removal.

Hein, Mai, and Barjenbruch (2011) analysed German Bight data similar to Wahl *et al*. (2011) using a similar approach, but they further develop the method through use of the second derivative to predict boundary values and calculate the white noise Monte Carlo simulation in the frequency space. By removing major frequency bands identified at approximately 35 and 75 years, Hein, Mai, and Barjenbruch (2011) concluded no evident long-term trend of acceleration in mean sea level around the German Bight.

Wahl *et al*. (2013) provides a detailed analysis of the North Sea regional sea-level records, updating the prior work of Shennan and Woodworth (1992) by considering three separate "regional sea-level indices" for the North Sea, Inner North Sea, and English Channel. This body of work concluded that recent rates of sea-level rise (*i.e*. over the last two to three decades) were high compared with the long-term average, but comparable to those observed at other times in the late 19th and 20th century. This investigation considers nonlinear (acceleration) behaviour using a similar technique to that espoused in Wahl *et al*. (2011).

Donner *et al*. (2012) provides a detailed examination of Baltic Sea records, examining measures of acceleration through the application of a fitted AR[1] model and performing separate (two-sided) t tests and Mann–Kendall tests for 1000 realisations of each model. This work observed that by comparing the empirical values of the test statistics with those obtained for AR[1] surrogates adjusted to the data, all accelerating trends in the 10% and 50% quantiles become insignificant with respect to both t and Mann–Kendall tests. Whilst seasonal influences appear to have been accounted for, there is no evidence that this approach is able to remove the contaminating decadal and multidecadal variability from the trends. Intuitively, this would increase the likelihood of statistically measured accelerations, but, in accordance with the approach and tests adopted, they were not realised. Despite differences in approaches, the current study also highlights the substantial absence of any periods of positive acceleration in mean sea level at the 95% confidence level across the Baltic Sea margin (Figure 6).

A detailed study of the Baltic mean sea-level records by Spada, Olivieri, and Galassi (2014) observed an anomaly in the long-term acceleration explained by classical postglacial rebound theory and numerical modelling of glacial isostasy. This work, however, is based upon the use of quadratic coefficients, which have significant limitations for the purpose at hand (Watson, 2016c). As previously advised, the current study finds no measureable acceleration in mean sea level within the Baltic Sea.

CONCLUSION

Watson (2016c) notes that the implications of sea-level rise, particularly the much larger projected rates of rise under future climate change modelled scenarios (*e.g.,* Church *et al.,* 2013; Mengel *et al.,* 2016), are profound, with far reaching social, economic, and environmental implications (amongst others) foreshadowed over the course of the 21st century and beyond. These are well described for the European context in the ClimateCost Project undertaken for the European Union (Brown *et al.,* 2011; Watkiss, 2011).

The effects across Europe associated with relative mean sea-level rise are quite varied, principally because of the associated vertical land motions, which range from high rates of land uplift associated with postglacial rebound experienced within the Fennoscandian region (up to ≈9 mm/y) to areas experiencing ongoing land subsidence (*e.g*., northern British Isles and the eastern portions of the Mediterranean and Black seas). Areas experiencing land subsidence will be affected more urgently and directly by rising global mean sea level. By contrast, depending on the trajectory of future sea-level rise, the northern land margins of Fennoscandia might still be rising faster than global mean sea level for the larger part of the 21st century, with no apparent issue for coast-dwelling communities until the rate of sea-level rise begins to overwhelm the rate of uplift from postglacial rebound.

Mean sea-level records are pivotal data sources because they provide one of the key proxies by which to measure a changing climate system. With the very ethos of climate change science and projection modelling underpinned by necessary and significant accelerations in mean sea level, numerous works in the scientific literature have been dedicated to measuring accelerations that might provide improved instruction on the future sea-level trajectory to assist strategic planning, adaptive responses, and policy development in readiness for the challenges ahead (Watson, 2016c).

Atlantic mean sea-level records could be considered one of the key "canaries in the coal mine" for climate change research given the North Atlantic Ocean is a key element of the Earth's climate (Deshayes and Frankignoul, 2008) and, in particular, the role of the AMOC as a key means by which heat anomalies are sequestered into the ocean's interior and thus modulate the trajectory of climate change (Buckley and Marshall, 2016).

The analytical techniques espoused in this paper improve estimates of mean sea level from conventional, long, annual time series by more efficiently removing decadal to interdecadal (and longer) dynamic influences. By virtue, associated kinematic properties of the mean sea-level signal (velocity, acceleration) are also enhanced.

In addition to the use of improved analytical techniques, the search for accelerations in mean sea-level records will require more intuitive, diagnostic considerations (such as those considered in this paper) until such time as the mean sea-level signal is sufficiently large not to be obscured by complex dynamic influences and other background noise.

Although the general tendency has been for velocity in mean sea level to increase over time, inferring an acceleration to do so, these kinematic properties of the mean sea level signal around Europe have continued to vary over the course of the historical records available at generally low measured rates. The analysis suggests key periods of acceleration centred in bands around ≈1880 to 1910, 1940, and 1976 and a strong spatially coherent signal between 1994 and 2000 consistent with the general findings of previous researchers using different techniques (*e.g.,* Wahl *et al.,* 2013; Woodworth *et al.,* 2009). Significantly, only one record within the study area exhibits a peak acceleration occurring after 1990 (Marseille, France) that is statistically different (or higher) from other peaks observed elsewhere over the historical record (95% confidence level).

Similarly only 5 of the 83 records analysed exhibited a peak velocity occurring after 1990 that was statistically different (or higher) than other peaks observed elsewhere over the historical record (95% confidence level). The Europe-wide context of these findings accord with the prior findings of studies on the English Channel (Haigh, Nicholls, and Wells, 2009) and North Sea (Dangendorf *et al*., 2014; Wahl *et al*., 2013).

When relative mean sea-level velocities are corrected for available vertical land motions, none of the geocentric velocities determined at the end of the available time series record exceed the global average rate of 3.4 ± 0.4 mm/y (CU Sea Level Research Group, 2016; Nerem *et al.,* 2010) at the 95% confidence level.

The results and findings from this large study of European mean sea-level records are broadly consistent with those for the complementary study of the mainland U.S. records (Watson, 2016c). Whilst the accelerated climate change influence is not yet statistically evident in these records, depending on the climate change trajectory, it is highly likely that such changes will take at least 15–20 years to manifest in the network of tide gauge records examined within this study.

ACKNOWLEDGMENTS

The author acknowledges the publicly available data archives of the PSMSL and the extended data sets provided by Peter Hogarth that have been used for this study. Similarly, the author extends thanks to the SONEL data centre for kindly providing the updated ULR6a solutions used to estimate geocentric sea-level rise in the paper. The author also thanks Dr. Sally Brown (Tyndall Centre for Climate Change Research, University of Southampton, U.K.) and Dr. Sönke Dangendorf (Research Institute for Water and Environment, University of Siegen, Germany) for suggestions that improved the paper.

LITERATURE CITED

Arabelos, D.N.; Papazachariou, D.Z.; Contadakis, M.E., and Spatalas, S.D., 2011. A new tide model for the Mediterranean Sea based on altimetry and tide gauge assimilation. *Ocean Science*, 7(3), 429–444.

Argus, D.F.; Peltier, W.R.; Drummond, R., and Moore, A.W., 2014. The Antarctica component of postglacial rebound model ICE-6G_C (VM5a) based on GPS positioning, exposure age dating of ice thicknesses, and relative sea level histories. *Geophysical Journal International*, 198(1), 537–563.

Avsar, N.B.; Jin, S.; Kutoglu, H., and Gurbuz, G., 2016. Sea level change along the Black Sea coast from satellite altimetry, tide gauge and GPS observations. *Geodesy and Geodynamics*, 7(1), 50–55.

Bakan, G. and Büyükgüngör, H., 2000. The Black Sea. *Marine Pollution Bulletin*, 41(1), 24–43.

Brown, S.; Nicholls, R.J.; Vafeidis, A.; Hinkel, J., and Watkiss, P., 2011. The impacts and economic costs of sea-level rise on coastal zones in the EU and the costs and benefits of adaptation. Summary of results from the EC RTD ClimateCost Project. *In:* Watkiss, P. (ed.), *The ClimateCost Project. Final Report. Volume 1: Europe*. Stockholm, Sweden: Stockholm Environment Institute, 43p.

Buckley, M.W. and Marshall, J., 2016. Observations, inferences, and mechanisms of the Atlantic meridional overturning circulation: A review. *Reviews of Geophysics*, 54(1), 5–63.

Bungenstock, F. and Schäfer, A., 2009. The Holocene relative sea-level curve for the tidal basin of the barrier island Langeoog, German Bight, southern North Sea. *Global and Planetary Change*, 66(1), 34–51.

Calafat, F.M. and Chambers, D.P., 2013. Quantifying recent acceleration in sea-level unrelated to internal climate variability. *Geophysical Research Letters*, 40(14), 3661–3666.

Calafat, F.M.; Chambers, D.P., and Tsimplis, M.N., 2012. Mechanisms of decadal sea level variability in the eastern North Atlantic and the Mediterranean Sea. *Journal of Geophysical Research: Oceans*, 117, C09022. doi:10.1029/2012JC008285

Chambers, D.P.; Merrifield, M.A., and Nerem, R.S., 2012. Is there a 60-year oscillation in global mean sea-level? *Geophysical Research Letters*, 39(18), L18801. doi:10.1029/2012GL052761

Church, J.A.; Clark, P.U.; Cazenave, A.; Gregory, J.M.; Jevrejeva, S.; Levermann, A.; Merrifield, M.A.; Milne, G.A.; Nerem, R.S.; Nunn, P.D.; Payne, A.J.; Pfeffer, W.T.; Stammer, D., and Unnikrishnan, A.S., 2013. Sea level change. *In:* Stocker, T.F.; Qin, D.; Plattner, G.-K.; Tignor, M.; Allen, S.K.; Boschung, J.; Nauels, A.; Xia, Y.; Bex, V., and Midgley, P.M. (eds.), *Climate Change 2013: The Physical Science Basis*. Contribution of Working Group I to the Fifth Assessment Report of the Intergovernmental Panel on Climate Change. Cambridge, U.K.: Cambridge University Press, pp. 1137–1216.

CU Sea Level Research Group, 2016. *Map of Sea Level Trends*. http://sealevel.colorado.edu/content/map-sea-level-trends.

Dangendorf, S.; Wahl, T.; Hein, H.; Jensen, J.; Mai, S., and Mudersbach, C., 2012. Mean sea level variability and influence of the North Atlantic Oscillation on long-term trends in the German Bight. *Water*, 4(1), 170–195.

Dangendorf, S.; Calafat, F.M.; Arns, A.; Wahl, T.; Haigh, I.D., and Jensen, J., 2014. Mean sea level variability in the North Sea: Processes and implications. *Journal of Geophysical Research: Oceans*, 119(10), 6820–6841.

Dangendorf, S.; Marcos, M.; Müller, A.; Zorita, E.; Riva, R.; Berk, K., and Jensen, J., 2015. Detecting anthropogenic footprints in sea level rise. *Nature Communications*, 6, 7849. doi:10.1038/ncomms8849

Deshayes, J. and Frankignoul, C., 2008. Simulated variability of the circulation in the North Atlantic from 1953 to 2003. *Journal of Climate*, 21(19), 4919–4933.

Donner, R.V.; Ehrcke, R.; Barbosa, S.M.; Wagner, J.; Donges, J.F., and Kurths, J., 2012. Spatial patterns of linear and nonparametric long-term trends in Baltic sea-level variability. *Nonlinear Processes in Geophysics*, 19(1), 95–111.

Douglas, B.C., 1992. Global sea-level acceleration. *Journal of Geophysical Research: Oceans*, 97(C8), 12699–12706.

Ericson, J.P.; Vörösmarty, C.J.; Dingman, S.L.; Ward, L.G., and Meybeck, M., 2006. Effective sea-level rise and deltas: Causes of change and human dimension implications. *Global and Planetary Change*, 50(1), 63–82.

Foster, G., and Brown, P.T., 2015. Time and tide: analysis of sea-level time series. *Climate Dynamics*, 45(1-2), 291–308.

Garcia, D.; Vigo, I.; Chao, B.F., and Martinez, M.C., 2007. Vertical crustal motion along the Mediterranean and Black Sea coast derived from ocean altimetry and tide gauge data. *Pure and Applied Geophysics*, 164(4), 851–863.

Getzlaff, J.; Böning, C.W.; Eden, C., and Biastoch, A., 2005. Signal propagation related to the North Atlantic overturning. *Geophysical Research Letters*, 32(9), L09602. doi:10.1029/2004GL021002

Golyandina, N. and Osipov, E., 2007. The "Caterpillar"-SSA method for analysis of time series with missing values. *Journal of Statistical Planning and Inference*, 137(8), 2642–2653.

Golyandina, N. and Zhigljavsky, A., 2013. *Singular Spectrum Analysis for Time Series*. Berlin, Heidelberg: Springer-Verlag, 120p.

Gomis, D.; Tsimplis, M.N.; Martín-Míguez, B.; Ratsimandresy, A.W.; García-Lafuente, J., and Josey, S.A., 2006. Mediterranean Sea level and barotropic flow through the Strait of Gibraltar for the period 1958–2001 and reconstructed since 1659. *Journal of Geophysical Research: Oceans*, 111, C11005. doi:10.1029/2005JC003186

Gomis, D.; Ruiz, S.; Sotillo, M.G.; Álvarez-Fanjul, E., and Terradas, J., 2008. Low frequency Mediterranean sea level variability: The contribution of atmospheric pressure and wind. *Global and Planetary Change*, 63(2), 215–229.

Goosse, H. and Renssen, H., 2005. A simulated reduction in Antarctic sea-ice area since 1750: Implications of the long memory of the ocean. *International Journal of Climatology*, 25(5), 569–579.

Goosse, H.; Masson-Delmotte, V.; Renssen, H.; Delmotte, M.; Fichefet, T.; Morgan, V.; Van Ommen, T.; Khim, B.K., and Stenni, B., 2004. A late medieval warm period in the Southern Ocean as a delayed response to external forcing? *Geophysical Research Letters*, 31, L06203. doi:10.1029/2003GL019140

Haigh, I.; Nicholls, R., and Wells, N., 2009. Mean sea level trends around the English Channel over the 20th century and their wider context. *Continental Shelf Research*, 29(17), 2083–2098.

Haigh, I.D.; Wahl, T.; Rohling, E.J.; Price, R.M.; Pattiaratchi, C.B.; Calafat, F.M., and Dangendorf, S., 2014. Timescales for detecting a significant acceleration in sea-level rise. *Nature Communications*, 5, 3635. doi:10.1038/ncomms4635

Hein, H.; Mai, S., and Barjenbruch, U., 2011. What tide gauges reveal about the future sea level. *Proceedings of the 4th Conference on Acqua Alta* (Hamburg, Germany), 9p.

Hogarth, P., 2014. Preliminary analysis of acceleration of sea-level rise through the twentieth century using extended tide gauge data sets (August 2014). *Journal of Geophysical Research: Oceans*, 119(11), 7645–7659.

Holgate, S.J.; Matthews, A.; Woodworth, P.L.; Rickards, L.J.; Tamisiea, M.E.; Bradshaw, E.; Foden, P.R.; Gordon, K.M.; Jevrejeva, S., and Pugh, J., 2012. New data systems and products at the permanent service for mean sea-level. *Journal of Coastal Research*, 29(3), 493–504.

IPCC (Intergovernmental Panel on Climate Change), 2013. Summary for policymakers. *In:* Stocker, T.F.; Qin, D.; Plattner, G.-K.; Tignor, M.; Allen, S.K.; Boschung, J.; Nauels, A.; Xia, Y.; Bex, V., and Midgley, P.M. (eds.), *Climate Change 2013: The Physical Science Basis*. Contribution of Working Group I to the Fifth Assessment Report of the Intergovernmental Panel on Climate Change. Cambridge, U.K.: Cambridge University Press, pp. 3–29.

Jevrejeva, S.; Moore, J.C.; Woodworth, P.L., and Grinsted, A., 2005. Influence of large-scale atmospheric circulation on European sea level: Results based on the wavelet transform method. *Tellus A*, 57(2), 183–193.

Kondrashov, D. and Ghil, M., 2006. Spatio-temporal filling of missing points in geophysical data sets. *Nonlinear Processes in Geophysics*, 13(2), 151–159.

Korotaev, G.; Oguz, T.; Nikiforov, A., and Koblinsky, C., 2003. Seasonal, interannual, and mesoscale variability of the Black Sea upper layer circulation derived from altimeter data. *Journal of Geophysical Research: Oceans*, 108(C4), 3122. doi:10.1029/2002JC001508

Kubryakov, A.A. and Stanichnyi, S.V., 2013. The Black Sea level trends from tide gages and satellite altimetry. *Russian Meteorology and Hydrology*, 38(5), 329–333.

Kullenberg, G., 1981. Physical oceanography. *In:* Voipio, A. (ed.), *The Baltic Sea*. Elsevier Oceanography Series 30. Amsterdam: Elsevier, pp. 135–182.

Lehmann, A.; Getzlaff, K., and Harla, J., 2011. Detailed assessment of climate variability of the Baltic Sea area for the period 1958–2009. *Climate Research*, 46(2), 185–196.

Leithe-Eriksen, R. (ed.), 1992. *The Seas of Europe—The Baltic Sea*. Ludwigsburg, Germany: RVG-Interbook, 144p.

Leppäranta, M. and Myrberg, K., 2009. *Physical Oceanography of the Baltic Sea*. Berlin, Heidelberg: Springer-Verlag, 378p.

Marcos, M.; Marzeion, B.; Dangendorf, S.; Slangen, A.B.; Palanisamy, H., and Fenoglio-Marc, L., 2016. Internal Variability Versus Anthropogenic Forcing on Sea Level and Its Components. *Surveys in Geophysics*. doi:10.1007/s10712-016-9373-3

McGranahan, G.; Balk, D., and Anderson, B., 2007. The rising tide: Assessing the risks of climate change and human settlements in low elevation coastal zones. *Environment and Urbanization*, 19(1), 17–37.

Meehl, G.A.; Stocker, T.F.; Collins, W.D.; Friedlingstein, P.; Gaye, A.T.; Gregory, J.M.; Kitoh, A.; Knutti, R.; Murphy, J.M.; Noda, A.; Raper, S.C.B.; Watterson, I.G.; Weaver, A.J., and Zhao, Z.-C., 2007. Global climate projections. *In:* Solomon, S.; Qin, D.; Manning, M.; Chen, Z.; Marquis, M.; Averyt, K.B.; Tignor, M., and Miller, H.L. (eds.), *Climate Change 2007: The Physical Science Basis*. Contribution of Working Group I to the Fourth Assessment Report of the Intergovernmental Panel on Climate Change. Cambridge, U.K.: Cambridge University Press, pp. 433–497.

Mengel, M.; Levermann, A.; Frieler, K.; Robinson, A.; Marzeion, B., and Winkelmann, R., 2016. Future sea level rise constrained by observations and long-term commitment. *Proceedings of the National Academy of Sciences*, 113(10), 2597–2602.

Minshull, T.A.; White, N.J.; Edwards, R.A.; Shillington, D.J.; Scott, C.L.; Demirer, A.; Shaw-Champion, M.; Jones, S.M.; Erduran, M.; Besevli, T., and Coskun, G., 2005. Seismic data reveal eastern Black Sea Basin structure. *EOS: Transactions American Geophysical Union*, 86(43), 413–419.

Moore, J.C.; Grinsted, A., and Jevrejeva, S., 2005. New tools for analyzing time series relationships and trends. *Eos, Transactions American Geophysical Union*, 86(24), 226–232.

Nerem, R.S.; Chambers, D.P.; Choe, C., and Mitchum, G.T., 2010. Estimating mean sea-level change from the TOPEX and Jason altimeter missions. *Marine Geodesy*, 33(S1), 435–446.

Neumann, B.; Vafeidis, A.T.; Zimmermann, J., and Nicholls, R.J., 2015. Future coastal population growth and exposure to sea-level rise and coastal flooding-a global assessment. *PLOS ONE*, 10(3), 0118571.

Nicholls, R.J. and Cazenave, A., 2010. Sea-level rise and its impact on coastal zones. *Science*, 328(5985), 1517–1520.

Panin, N. and Jipa, D., 2002. Danube River sediment input and its interaction with the north-western Black Sea. *Estuarine, Coastal and Shelf Science*, 54(3), 551–562.

Peltier, W.R.; Argus, D.F., and Drummond, R., 2015. Space geodesy constrains ice age terminal deglaciation: The global ICE-6G_C (VM5a) model. *Journal of Geophysical Research: Solid Earth*, 120(1), 450–487.

PSMSL (Permanent Service for Mean Sea-Level), 2016. http://www.psmsl.org.

Pugh, D.T., 1996. *Tides, Surges and Mean Sea-Level* (reprinted with corrections). Chichester, U.K.: John Wiley & Sons, 486p.

Qiu, B. and Chen, S., 2012. Multidecadal sea-level and gyre circulation variability in the northwestern tropical Pacific Ocean. *Journal of Physical Oceanography*, 42(1), 193–206.

R Development Core Team, 2015. *R: A Language and Environment for Statistical Computing*. Vienna, Austria: R Foundation for Statistical Computing. http://www.R-project.org.

Santamaría-Gómez, A.; Gravelle, M.; Collilieux, X.; Guichard, M.; Míguez, B.M.; Tiphaneau, P., and Wöppelmann, G., 2012. Mitigating the effects of vertical land motion in tide gauge records using a state-of-the-art GPS velocity field. *Global and Planetary Change*, 98, 6–17.

Shennan, I. and Woodworth, P.L., 1992. A comparison of late Holocene and twentieth-century sea-level trends from the UK and North Sea region. *Geophysical Journal International*, 109(1), 96–105.

Smith, K., 2011. We are seven billion. *Nature Climate Change*, 1(7), 331–335.

Spada, G.; Olivieri, M., and Galassi, G., 2014. Anomalous secular sea-level acceleration in the Baltic Sea caused by isostatic adjustment. *Annals of Geophysics*, 57(4), S0432. doi:10.4401/ag-6548

Stanev, E.V., 2005. Black Sea dynamics. *Oceanography*, 18(2), 56–75.

Sturges, W. and Douglas, B.C., 2011. Wind effects on estimates of sea-level rise. *Journal of Geophysical Research: Oceans*, 116, C06008. doi:10.1029/2010JC006492

SONEL (Systeme d'Observation du Niveau des Eaux Littorales), 2016. http://www.sonel.org/-Vertical-land-movement-estimate-.html.

Trenberth, K.E. and Hurrell, J.W., 1994. Decadal atmosphere-ocean variations in the Pacific. *Climate Dynamics*, 9(6), 303–319.

Tsimplis, M.; Marcos, M.; Somot, S., and Barnier, B., 2008. Sea level forcing in the Mediterranean Sea between 1960 and 2000. *Global and Planetary Change*, 63(4), 325–332.

Tsimplis, M.N. and Shaw, A.G., 2008. The forcing of mean sea level variability around Europe. *Global and Planetary Change*, 63(2), 196–202.

Tsimplis, M.N.; Shaw, A.G.P.; Flather, R.A., and Woolf, D.K., 2006. The influence of the North Atlantic Oscillation on the sea-level around the northern European coasts reconsidered: The thermosteric effects. *Philosophical Transactions of the Royal Society A*, 364(1841), 845–856.

Vigo, I.; Garcia, D., and Chao, B.F., 2005. Change of sea level trend in the Mediterranean and Black seas. *Journal of Marine Research*, 63(6), 1085–1100.

Volkov, D.L. and Landerer, F.W., 2015. Internal and external forcing of sea level variability in the Black Sea. *Climate Dynamics*, 45(9-10), 2633–2646.

Wahl, T.; Jensen, J., and Frank, T., 2010. On analysing sea level rise in the German Bight since 1844. *Natural Hazards and Earth System Science*, 10(2), 171–179.

Wahl, T.; Jensen, J.; Frank, T., and Haigh, I.D., 2011. Improved estimates of mean sea level changes in the German Bight over the last 166 years. *Ocean Dynamics*, 61(5), 701–715.

Wahl, T.; Haigh, I.D.; Woodworth, P.L.; Albrecht, F.; Dillingh, D.; Jensen, J.; Nicholls, R.J.; Weisse, R., and Wöppelmann, G., 2013. Observed mean sea level changes around the North Sea coastline from 1800 to present. *Earth-Science Reviews*, 124, 51–67.

Wakelin, S.L.; Woodworth, P.L.; Flather, R.A., and Williams, J.A., 2003. Sea-level dependence on the NAO over the NW European Continental Shelf. *Geophysical Research Letters*, 30(7), 1403.

Watkiss, P., 2011. *The ClimateCost Project. Final Report, Volume 1: Europe*. Stockholm, Sweden: Stockholm Environmental Institute.

Watson, P.J., 2015. Development of a unique synthetic data set to improve sea-level research and understanding. *Journal of Coastal Research*, 31(3), 758–770.

Watson, P.J., 2016a. Identifying the best performing time series analytics for sea-level research. *In:* Rojas, I. and Pomares, H. (eds.), *Time Series Analysis and Forecasting: Contributions to Statistics*. Cham, Switzerland: Springer International, pp. 261–278.

Watson, P.J., 2016b. How to improve estimates of real-time acceleration in the mean sea-level signal. *In:* Vila-Concejo, A.; Bruce, E.; Kennedy, D.M., and McCarroll, R.J. (eds.), *Proceedings of the 14th International Coastal Symposium*. *Journal of Coastal Research*, Special Issue, No. 75, pp. 780–784.

Watson, P.J., 2016c. Acceleration in USA mean sea-level? A new insight using improved tools. *Journal of Coastal Research*. In press. doi:10.2112/JCOASTRES-D-16-00086.1

Wolfe, R. and Hanley, J., 2002. If we're so different, why do we keep overlapping? When 1 plus 1 doesn't make 2. *Canadian Medical Association Journal*, 166(1), 65–66.

Woodworth, P.; White, N.J.; Jevrejeva, S.; Holgate, S.; Church, J., and Gehrels, W., 2009. Evidence for the accelerations of sea-level on multi-decade and century timescales. *International Journal of Climatology*, 29(6), 777–789.

Woodworth, P.L., 1990. A search for accelerations in records of European mean sea-level. *International Journal of Climatology*, 10(2), 129–143.

Woolf, D.K.; Shaw, A.G.P., and Tsimplis, M.N., 2003. The influence of the North Atlantic Oscillation on sea level variability in the North Atlantic Region. *The Global Atmosphere and Ocean System*, 9(4), 145–167.

Yan, Z.; Tsimplis, M.N., and Woolf, D., 2004. An analysis of relationship between the North Atlantic Oscillation and sea level changes in NW Europe. *International Journal of Climatology*, 24, 743–758.